Materials Physics and Mechanics. 2023;51(3): 20-28
Research article
http://dx.doi.org/10.18149/MPM.5132023_3

Submitted: November 23, 2022
Approved: February 25, 2023
Accepted: March 30, 2023

Effect of annealing and additional deformation on the microstructure and mechanical properties of ultrafine-grained Al5083 alloy

A.D. Evstifeev [1,2] ✉, **I.V. Smirnov** [1]

[1] Saint Petersburg State University, Saint Petersburg, Russia

[2] National Research Lobachevsky State University of Nizhny Novgorod, Nizhny Novgorod, Russia

✉ ad.evstifeev@gmail.com

Abstract. The microstructure and mechanical properties of ultrafine-grained (UFG) aluminum alloy Al5083 in different structural states were investigated. The UFG structure was formed by high-pressure torsion (HPT) technique. The UFG alloy exhibits high value of ultimate tensile strength (~ 725 MPa) but no ductility. Short-term annealing at 473 K and additional deformation by HPT to 0.25 of revolution at room temperature resulted in a slight decrease in material's strength to ~ 653 MPa, which was ~ 90 % of the value after HPT processing but provided ductility ~ 2 %. Microstructure evolution during deformation heat treatment was investigated by transmission electron microscopy and X-ray diffraction analysis. Physical mechanisms to improve plasticity in correlation with microstructure evolution is discussed.

Keywords: aluminum-magnesium alloys, severe plastic deformation, strength, ductility, microstructure, ultrafine-grained structure

Acknowledgements. *The study funded by grant № 19-31-60031 from the Russian Foundation for Basic Research.*

Citation: Evstifeev AD, Smirnov IV. Effect of annealing and additional deformation on the microstructure and mechanical properties of ultrafine-grained Al5083 alloy. *Materials Physics and Mechanics*. 2023;51(3): 20-28. DOI: 10.18149/MPM.5132023_3.

Introduction

Aluminum alloys due to their high strength and performance characteristics have extensive application in the industry as a stamping and casting material. Al-Mg alloys are characterized by good weldability and high corrosion resistance in the atmosphere as well as in saltwater [1,2]. Mg content increasing up to 6% results in the strengthening of the alloys, at the same time it reduces the alloy's ductile properties and corrosion resistance [1]. Besides alloying, Al-Mg series can be a strain hardened, but practically not strengthened by heat treatment [2].

Severe plastic deformation (SPD) allows the formation of unique microstructure and properties in bulk metallic materials [3,4]. Various SPD methods have been developed and examined in recent years, the results of this investigations have been analyzed and summarized in recent reviews [3,5–8].

To date, the greatest interest has been focused on two SPD methods: equal-channel angular pressing (ECAP) and high-pressure torsion (HPT) [6–9]. ECAP is relatively easy-to-implement method allowing to obtain bulk metallic samples which can be studied by standard mechanical tests. At the same time, HPT method, in comparison with ECAP, allows to create

Publisher: Peter the Great St. Petersburg Polytechnic University

materials with smaller mean grain size and higher degree of grain boundary misorientation [10]. In recent years, many studies have been performed on SPD-processed pure aluminum and aluminum-based alloys [11–18]. It was shown that SPD processing results in formation ultrafine-grained (UFG) structure providing high mechanical strength. Furthermore, in some cases, materials with enhanced mechanical strength demonstrate high ductility [17–18], although this is mutually exclusive properties for traditional metallic materials [19]. In [18] a new approach to improve plasticity while maintaining high strength of HPT-processed commercially pure Al was proposed. This approach is based on the modification of the annealed structure of the high-angle grain boundaries by a slight additional deformation by HPT after short-term low-temperature annealing.

As it was shown for ECAP processed Al–Mg alloys, increase in Mg content from 0.5 to 2 wt.% leads to grain grinding and increase in dislocation density [20]. The UFG Al–Mg alloys produced by HPT retained ductility at the acceptable level while Mg content is less than 2.5 wt.% [21]. Further increase in Mg content up to 4.1 wt.% results in decrease of ductility of HPT-processed alloy [22]. The increase of Mg content up to 4.5 wt.% completely suppresses plastic deformation in the HPT-processed material [21–22]. Thermal stability of nanostructured Al–Mg alloys remains unclear. One study found that Al–5Mg (wt.%) alloy treated by surface mechanical grinding has enhanced thermal stability of mechanical properties up to 475 K [23]. Another study found degradation of mechanical properties of Al–5.5Mg (wt.%) alloy produced by ECAP with an increase in the annealing duration at 623 K [24].

In this study the possibility of simultaneous increase in strength and ductility of the HPT-processed Al5083 commercial alloy by additional deformation heat treatment previously proposed in [18] was investigated.

Material and experimental methods

Al5083 commercial alloy (4.56Mg; 0.46Mn; 0.32Fe; 0.21Si wt.% in Al balance) was chosen in this study. The initial material was in a cast state. The structure was modified on the Walter-Klement HPT press to 10 revolutions at room temperature (RT) under a pressure of 6 GPa. After HPT processing disks with a diameter of 20 mm and thickness of 1.6 mm were formed. The logarithmic strain of material at the middle of the disk radius was $e \approx 5.5$ [25]. Additional deformation heat treatment included annealing at 333–723 K for 1 h and further HPT processing to 0.25 revolutions at RT under the same pressure, which corresponded to the extra logarithmic strain of $e \approx 1.5$ [25].

The microstructure of the material was studied by transmission electron microscopy (TEM) and X-ray diffraction analysis (XRD). The TEM studies were performed on a Zeiss Libra 200FE microscope. Thin foils for TEM observation were prepared by mechanical polishing followed by double-jet electropolishing. XRD analysis was performed on a Bruker D8 DISCOVER diffractometer in a symmetric θ–2θ scan modes using a parallel beam of CuKα radiation (40 kV, 40 mA). The scanning step was $\Delta 2\theta = 0.02°$ and the time of exposure was 0.5 s. The average size of the coherent scattering regions (C) and the level of microdistortion of the crystal lattice ($\langle \varepsilon^2 \rangle^{1/2}$) were determined via the full-profile Pauli simulation using the TOPAS 5.0 software. The dislocation density was calculated according to the following ratio [26]:

$$L_{dis} = \frac{2\sqrt{3}\langle \varepsilon^2 \rangle^{1/2}}{Cb}, \quad (1)$$

where b = 0.286 nm is the Burgers vector for edge dislocation in Al.

The microhardness (HV) of the samples was measured via the Vickers method on a Shimadzu HMV-G21DT test machine. In addition, uniaxial tensile tests were performed at a constant strain rate of $5 \cdot 10^{-4}$ s^{-1}. Dog-bone samples with the gauge length of 5 mm and width

of 2 mm were cut. According to the tensile tests, the average values of the yield stress ($\sigma_{0.2}$) corresponding to 0.2 % of deformation, the ultimate tensile strength (σ_{UTS}), the relative elongation to failure (δ), and the relative uniform elongation (δ_1) were determined. Fracture surfaces of the destroyed samples were studied using the scanning electron microscope (SEM) Zeiss AURIGA at the accelerating voltage of 10 kV.

Experimental results and discussion

The stress-strain curves for Al5083 samples in different states are shown on Fig. 1. The initial state characterized by low tensile strength ($\sigma_{UTS} \approx 240$ MPa) and high elongation to failure $\delta \approx 10$ % (curve 1 on Fig. 1). After HPT processing the ultimate strength of the material has tripled from ~ 240 to ~ 723 MPa, at the same time, samples demonstrated brittle behavior (curve 2 on Fig. 1). Microhardness of the material has tripled from ~ 780 to ~ 2180 MPa during HPT processing as well (Fig. 2(a)). Subsequent annealing of the HPT-processed material at temperatures up to 473 K results in minor decrease in microhardness (Fig. 2(a)). Further elevation of annealing temperature up to 623 K leads to the softening of the material as well as to rise in elongation (Fig. 2(b)). In the temperature range 473–523 K the microhardness decreased sharply (Fig. 2(a)). After annealing of at 473 K the ultimate tensile strength of the material was ~ 518 MPa, but there was no plastic deformation during tension (curve 3 on Fig. 1). The results of the mechanical tests of the material in different structural states are summarized in Table 1.

Table 1. Mechanical properties of the Al5083 alloy in different structural states. *HV* is the microhardness, $\sigma_{0.2}$ is the yield stress, corresponding to 0.2 % of deformation, σ_{UTS} is the ultimate tensile strength, δ is the relative elongation to failure, δ_1 is the relative uniform elongation

State	*HV*, MPa	$\sigma_{0.2}$, MPa	σ_{UTS}, MPa	δ, %	δ_1, %
Initial	780±3	120±2	240±5	11	8.8
HPT	2180±8	725±1	725±2	0	0
HPT + annealing at 473 K	1990±15	518±2	518±5	0	0
HPT + annealing at 473 K + HPT to 0.25 of revolution	1950±14	329±1	653±3	2	2

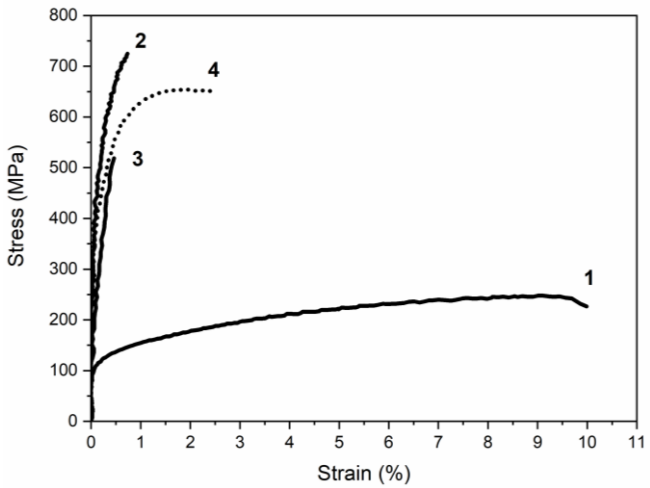

Fig. 1. Stress-strain diagrams of Al5083 in initial state (1), after HPT processing (2), after HPT processing and annealing at 473 K for 1 h (3), after HPT processing, annealing at 473 K for 1 h and additional HPT deformation to 0.25 revolutions (4)

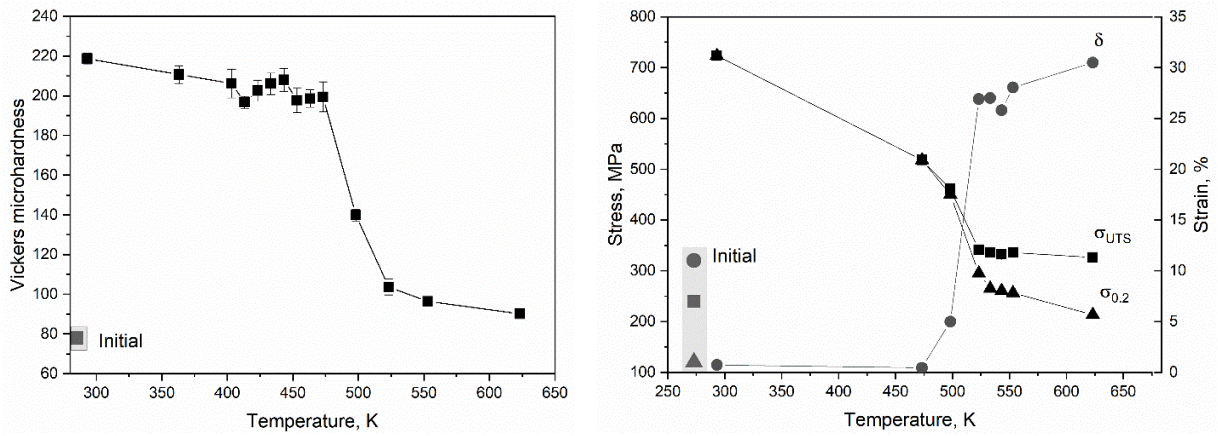

(a) (b)

Fig. 2. (a) Microhardness dependance; (b) ultimate tensile strength, yield stress, and elongation to failure dependences of the HPT processed Al5083 alloy on annealing temperature

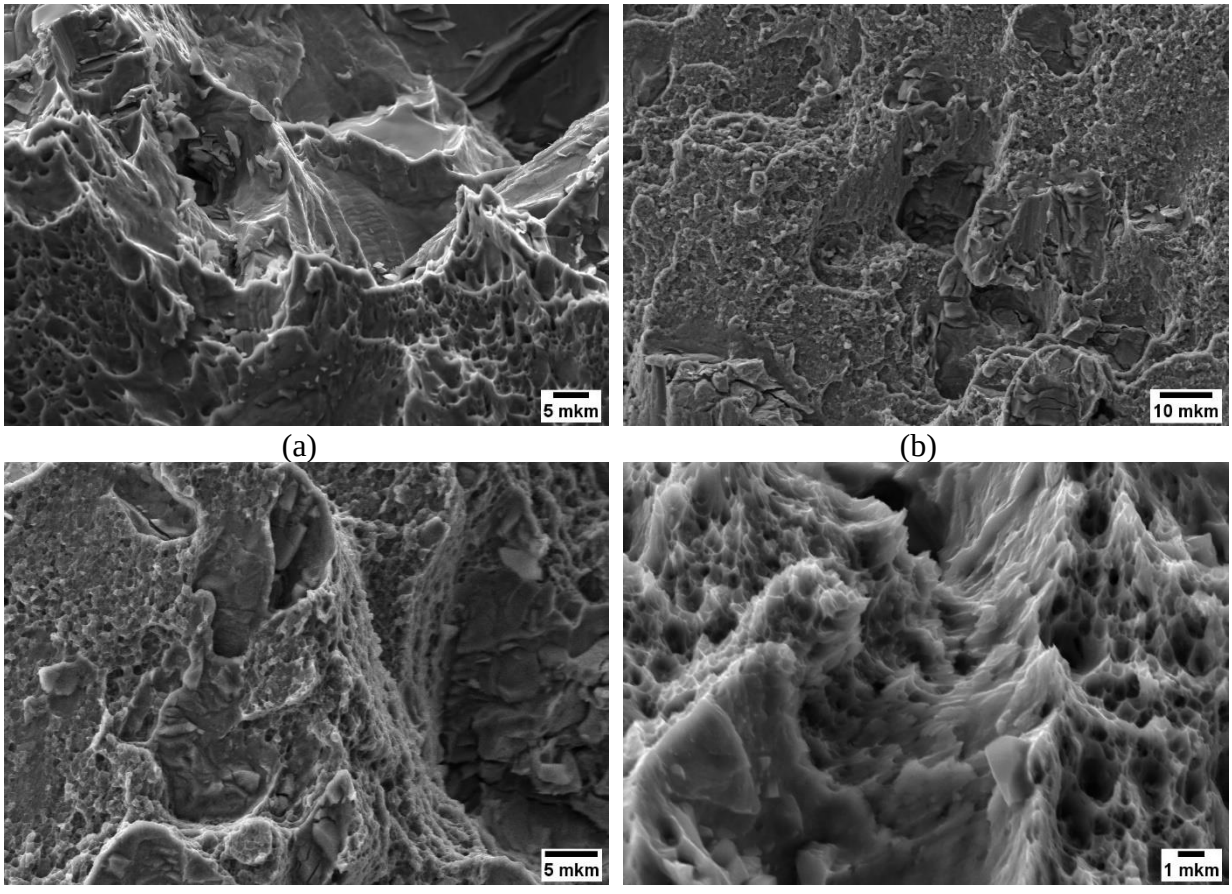

(a) (b)

(c) (d)

Fig. 3. Fracture surface of the Al5083 alloy in initial state (a), after HPT processing (b), after HPT processing and annealing at 473 K for 1 h (c), after HPT processing, annealing at 473 K for 1 h and additional HPT deformation to 0.25 revolutions (d)

The fracture surface of the initial material has an extensive zone of plastic deformation with a strongly pronounced relief structure (Fig. 3(a)). The fracture surface of the HPT-processed material is shown on Fig. 3(b). As it is seen the relief of the surface is less pronounced: along with large pits there are smooth areas which is linear with the brittle behavior of the stress-strain curve and obtained fining of grain structure. The fracture surface

of sample after HPT processing and annealing at 473 K is characterized by a brittle fracture with an extensive net of cracks along the surface of the working part of the sample (Fig. 3(c)). There are no obvious traces of plastic deformation on the cracked surface.

A threshold heat treatment that corresponds to annealing of the deformed material at 473 K for 1 h was selected to additional deformation by HPT to 0.25 revolutions as it was proposed to commercially pure Al as an effective way to improve ductile properties [18]. As a result, an increase in the material's ultimate tensile strength from ~ 518 MPa to ~ 653 MPa and elongation to failure of 2 % were obtained (curve 4 on Fig. 1, Table 1). The fracture surface of samples after HPT, annealing and additional HPT processing is shown in Fig. 2(d). The fracture surface has, in addition to signs of brittle fracture, areas of plastic deformation in the form of pit failure formed by the nucleation and fusion of micropores. Also, there are no microcracks on the fracture surface.

According to X-ray analysis annealing of HPT-processed sample leads to a significant decrease in the microdistortions of the crystalline lattice and enlargement of coherent scattering domains. Corresponding decrease in dislocation density can be estimated based on ratio (1). An additional HPT processing of the annealed structure resulted in a six-fold increase in the dislocation density from $1.1 \cdot 10^{13}$ to $6.4 \cdot 10^{13}$ m^{-2} (Table 2). Figure 4(a,b) shows TEM images for the HPT-processed material after annealing at 473 K and annealing and additional HPT processing. Structure of both samples is represented by equiaxed grains. Additional deformation of the partially relaxed (by annealing) material results in fining of the material's grain structure: the average grain size decreases from ~ 191 to ~ 135 nm which is well illustrated on the corresponding diagrams of grain size distribution (Fig. 4(c,d)). The TEM micrographs show that the grain interiors free from dislocation for both samples. It is most likely that the deformation-induced dislocation density was concentrated at the grain boundaries or near-grain boundary areas. This is also supported by fractography data, which did not reveal any obvious signs of intergranular destruction.

The microstructural parameters obtained (Table 2) serve as a basis to estimate these hardening contributions according to the relations [27–29]:

$$\sigma_{GB} = K d_{av}^{-1/2}, \tag{2}$$

$$\sigma_{dis} = M \alpha G b L_{dis}^{1/2}, \tag{3}$$

where: K = 0.1 MPa m^{-1} is the Hall-Petch coefficient [30], d_{av} is the average grain size, M = 3.06 is the Taylor factor [29], α = 0.33 is the dislocation interaction parameter [31], G = 26 GPa is the shear modulus.

According to (2) and (3) decrease in average grain size and dislocation density increase during additional HPT processing leads to strengthening by ~ 43 MPa and ~ 35 MPa, correspondingly. However, the sum of these estimates is smaller than experimentally obtained strengthening $\Delta\sigma_{0.2}$ = 190 MPa (Table 1). Our evaluations indicate that other strengthening mechanisms are possible in the examined material. For example, in [32–36] it was shown that in various SPD-processed aluminum alloys there is an additional contribution to strengthening due to the presence of grain boundary segregations. The only explanation of manifestation of plastic properties after additional HPT processing can be given on the bases of the model proposed earlier in [37]: the deformation-induced dislocations are formed in a dislocation pile-ups in triple junctions of high-angle grain boundaries; plastic deformation occurs through the emission of lattice dislocations from triple junctions of grain boundaries, the glide of the lattice dislocations across neighboring grains, their accumulation at and climb along the opposite grain boundaries.

Table 2. Microstructure parameters of the Al5083 alloy in different structural states. d_{av} is the average grain size, C is the size of coherent-scattering domains, $\langle\varepsilon^2\rangle^{1/2}$ is the elastic microdistortions level, L_{dis} is the dislocation density

State	d_{av}, nm	C, nm	$\langle\varepsilon^2\rangle^{1/2}$	$L_{dis}\cdot10^{13}$, m^{-2}
Initial	-	-	0.00016	-
HPT	-	20	0.00084	9.4
HPT + annealing at 473 K	191	203	0.00018	1.1
HPT + annealing at 473 K + HPT to 0.25 of revolution	135	139	0.0007	6.4

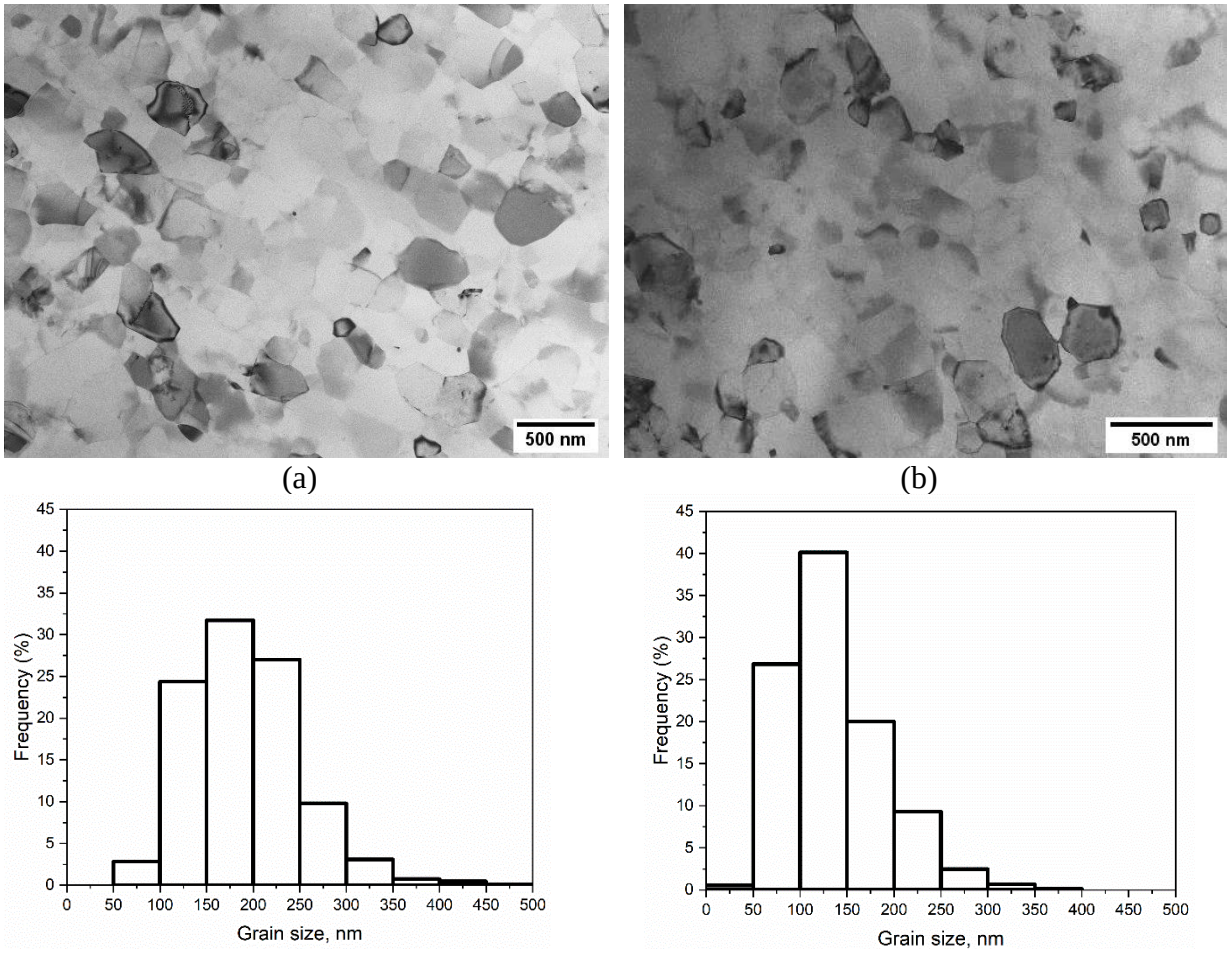

Fig. 4. TEM micrographs of the HPT-processed Al5083 alloy after annealing at 473K (a), annealing at 473 K and addition deformation by HPT to 0.25 of revolution (b) and corresponding grain size distribution (c), (d)

Conclusions

HPT processing of the commercial aluminum alloy 5083 significantly increased the ultimate tensile strength of the material by ~ 3 times while its ductility suffered. An increase in ductility (up to ~ 2 %), while maintaining a high tensile strength, was obtained by additional deformation and heat treatment, which included annealing at 473 K for 1 h and HPT processing to 0.25 of revolution. TEM analysis of UFG material does not reveal intergranular dislocations which is in line with the results of fractography indicating a lack of intergranular destruction. The obtained combination of sufficient ductility (~ 2 %) and high tensile strength (~ 653 MPa) was obtained by introducing of an additional dislocation density into the grain

boundary or near grain boundary structure. The proposed approach suggests high potential for practical applications of the alloy studied and can be a universally effective way to achieve a combination of high strength and ductility for various UFG materials.

References

1. Mondolfo LF. *Aluminum alloys: structure and properties*. Elsevier; 2013.
2. *Aluminum Association. Aluminum: properties and physical metallurgy*. ASM International; 1984.
3. Zhu Y, Valiev RZ, Langdon TG, Tsuji N, Lu K. Processing of nanostructured metals and alloys via plastic deformation. *MRS Bulletin*. 2010;35: 977–981.
4. Rudskoi AI, Bogatov AA, Nukhov DSh, Tolkushkin AO, On the development of the new technology of severe plastic deformation in metal forming. *Materials Physics and Mechanics.* 2018;38(1): 76-81.
5. Estrin Y, Vinogradov A. Extreme grain refinement by severe plastic deformation: A wealth of challenging science. *Acta Mater.* 2013;61(3): 782-817.
6. Langdon TG. Twenty-five years of ultrafine-grained materials: Achieving exceptional properties through grain refinement. *Acta Mater*. 2013;61(19): 7035-7059.
7. Sabirov I, Murashkin MY, Valiev RZ. Nanostructured aluminium alloys produced by severe plastic deformation: New horizons in development. *Materials Science & Engineering A*. 2013;560(10): 1-24.
8. Kawasaki M, Langdon TG. Review: achieving superplasticity in metals processed by high-pressure torsion. *J. Mater. Sci*. 2014;49: 6487–6496.
9. Rudskoi AI, Zolotov AM, Parshikov RA, Severe plastic deformation influence on engineering plasticity of Copper. *Materials Physics and Mechanics.* 2018;38(1): 64-68.
10. Wongsa-Ngam J, Kawasaki M, Langdon TG. A comparison of microstructures and mechanical properties in a Cu–Zr alloy processed using different SPD techniques. *J. Mater. Sci*. 2013;48: 4653–4660.
11. Duchaussoy A, Sauvage X, Edalati K, Horita Z, Renou G, Deschamps A, De Geuser F. Structure and mechanical behavior of ultrafine-grained aluminum-iron alloy stabilized by nanoscaled intermetallic particles. *Acta Mater*. 2019;167: 89–102.
12. Talebanpour B, Ebrahimi R, Janghorban K. Microstructural and mechanical properties of commercially pure aluminum subjected to Dual Equal Channel Lateral Extrusion. *Mater. Sci. Eng. A.* 2009;527(1-2): 141-145.
13. Sabirov I, Murashkin MY, Valiev RZ. Nanostructured aluminium alloys produced by severe plastic deformation: New horizons in development. *Mater. Sci. Eng. A.* 2013;560: 1-24.
14. Mavlyutov AM, Bondarenko AS, Murashkin MY, Boltynjuk EV, Valiev RZ, Orlova TS. Effect of annealing on microhardness and electrical resistivity of nanostructured SPD aluminium. *J. Alloys Comp*. 2017;698: 539–546.
15. Mavlyutov AM, Kasatkin IA, Murashkin MY, Valiev RZ, Orlova TS. Influence of the microstructure on the physicomechanical properties of the aluminum alloy Al–Mg–Si nanostructured under severe plastic deformation. *Phys. Solid State*. 2015;57: 2051–2058.
16. Huang X, Hansen N, Tsuji N. Hardening by annealing and softening by deformation in nanostructured metals. *Science*. 2006;312(5771): 249-251.
17. Kamikawa N, Huang X, Tsuji N, Hansen N. Strengthening mechanisms in nanostructured high-purity aluminium deformed to high strain and annealed. *Acta Materialia*. 2009;57(14): 4198-4208.
18. Mavlyutov AM, Latynina TA, Murashkin MY, Valiev RZ, Orlova TS. Effect of annealing on the microstructure and mechanical properties of ultrafine-grained commercially pure Al. *Phys. Solid State*. 2017;59: 1970–1977.

19. Valiev RZ, Alexandrov IV, Zhu YT, Lowe TC. Paradox of Strength and Ductility in Metals Processed by Severe Plastic Deformation. *Journal of Materials Research*. 2002;17: 5–8.
20. Kalsar R, Yadav D, Sharma A, Brokmeier HG, May J, Höppel HW, Skrotzki W, Suwas S. Effect of Mg content on microstructure, texture and strength of severely equal channel angular pressed aluminium-magnesium alloys. *Mater. Sci. Eng. A*. 2020;797: 140088.
21. Liu MP, Roven HJ, Murashkin MY, Valiev RZ, Kilmametov A, Zhang Z, Yu Y. Structure and mechanical properties of nanostructured Al-Mg alloys processed by severe plastic deformation. *J. Mater. Sci*. 2013;48: 4681-4688.
22. Liu Y, Liu M, Chen X, Cao Y, Roven HJ, Murashkin M, Zhou H. Effect of Mg on microstructure and mechanical properties of Al-Mg alloys produced by high pressure torsion. *Scripta Materialia*. 2019;159: 137-141.
23. Xu W, Zhang B, Du K, Li XY, Lu K. Thermally stable nanostructured Al-Mg alloy with relaxed grain boundaries. *Acta Mater*. 2022;226: 117640.
24. Snopiński P, Tański T. Thermal stability and microstructure evolution of ultra-fine grained Al-Mg alloy. *IOP: Conference Series*. 2018;461: 012085.
25. Zhilyaev AP, Langdon TG. Using high-pressure torsion for metal processing: Fundamentals and applications. *Progress in Materials Science*. 2008;53(6): 893-979.
26. Williamson GK, Smallman RE. III. Dislocation densities in some annealed and cold-worked metals from measurements on the X-ray debye-scherrer spectrum. *Phil. Mag*. 1956;1(1): 34-46.
27. Hall EO. The Deformation and Ageing of Mild Steel: III Discussion of Results. *Proceedings of the Physical Society. Section B*. 1951;64(9): 747.
28. Petch NJ. The orientation relationships between cementite and α-iron. *Acta Crystallographica*. 1953;6(1): 96-96.
29. Hansen N, Huang X. Microstructure and flow stress of polycrystals and single crystals. *Acta Materialia.* 1998;46(5): 1827-1836.
30. Totten GE, MacKenzie DS. *Handbook of Aluminium*. New York: Marcel Dekker; 2003.
31. Nabarro FRN, Basinski ZS, Holt DB. The plasticity of pure single crystals. *Adv. Phys.* 1964;13(50): 193-323.
32. Valiev RZ, Enikeev NA, Murashkin MY, Kazykhanov VU, Sauvage X. On the origin of the extremely high strength of ultrafinegrained Al alloys produced by severe plastic deformation. *Scripta Materialia*. 2010;63(9): 949-952.
33. Sauvage X, Ganeev A, Ivanisenko Y, Enikeev N, Murashkin M, Valiev R. Grain boundary segregation in UFG alloys processed by severe plastic deformation. *Advanced Engineering Materials*. 2012;14(11): 968-974.
34. Valiev RZ. Superior Strength in Ultrafine-Grained Materials Produced by SPD Processing. *Materials Transactions*. 2014; 55(1): 13-18.
35. Sauvage X, Murashkin MY, Valiev RZ. Atomic scale investigation of dynamic precipitation and grain boundary segregation in a 6061 aluminium alloy nanostructured by ECAP. *Kovove Mater*. 2011; 49(1): 11-15.
36. Pun SC, Wang W, Khalajhedayati A, Schuler JD, Trelewicz JR, Rupert TJ. Nanocrystalline Al-Mg with extreme strength due to grain boundary doping. *Mater. Sci. Eng. A*. 2017; 696: 400–406.
37. Orlova TS, Skiba NV, Mavlyutov AM, Murashkin MY, Valiev RZ, Gutkin MY. Hardening by annealing and implementation of high ductility of ultra-fine grained aluminum: experiment and theory. *Reviews on Advanced Materials Science*. 2018; 57(2): 224-240.

THE AUTHORS

A.D. Evstifeev
e-mail: ad.evstifeev@gmail.com

I.V. Smirnov
e-mail: i.v.smirnov@spbu.ru